Mon. Not. R. Astron. Soc. **000**, 000–000 (0000) Printed 7 December 2015 (MN LATEX style file v2.2)

The accretion regimes of a highly magnetised NS: the unique case of NuSTAR J095551+6940.8

Simone Dall'Osso[1], Rosalba Perna[1], Alessandro Papitto[2], Enrico Bozzo[3], Luigi Stella[4]
[1] *Department of Physics and Astronomy, Stony Brook University, Stony Brook, NY, USA*
[2] *Institute of Space Sciences (ICE, CSICIEEC), Carrer de Can Magrans, S/N, E-08193 Barcelona, Spain*
[3] *ISDC, University of Geneva, Chemin d'Ecogia 16, CH-1290 Versoix, Switzerland*
[4] *INAF - Osservatorio Astronomico di Roma, via di Frascati 33, 00044, Monteporzio Catone, Roma, Italy*

arXiv:1512.01532v1 [astro-ph.HE] 4 Dec 2015

7 December 2015

ABSTRACT

We analyze archival Chandra HRC observations of the ultraluminous accreting pulsar M82-X2 (NuSTAR J095551+6940.8), determining an upper limit of $< 1.7 \times 10^{38}$ erg s^{-1} to its luminosity at an epoch at which it was undetected. Combined with other recent measurements, this confirms that the source X-ray emission has been highly variable during the last 15 years, ranging from a maximum of 10^{40} erg s^{-1}through intermediate values $\sim$ a few $\times 10^{39}$ erg s^{-1}, and down to a minimum that must be below the current detection threshold $\sim 2 \times 10^{38}$ erg s^{-1}. We interpret these results by means of a magnetically-threaded disk model: when at peak luminosity, the neutron star (NS) is close to spin equilibrium, its inner disk edge $r_m \sim 10^8$ cm is approximately half the corotation radius r_{co}, and radiation pressure dominates the disk out to $r_{tr} \lesssim 10^9$ cm. In the radiation pressure-dominated regime, r_m grows very slowly as the mass inflow rate drops: as a result, $r_m < r_{co}$ remains valid until $\dot{M} \gtrsim \dot{M}_E$, the Eddington accretion rate, allowing a wide range of accretion luminosities to the NS. Once $\dot{M} < \dot{M}_E$ accretion onto the NS is inhibited because $r_m > r_{co}$, and the source luminosity is expected to drop by a large factor. We conclude that a magnetically threaded, radiation pressure-dominated disk, around a highly magnetized NS ($B \lesssim 10^{13}$ G) offers the best intepretation for all the currently observed properties of NuSTAR J095551+6940.8. This source offers an unprecedented opportunity to study the disk-magnetosphere interaction in a new regime of supercritical accretion, and across the transition between-radiation pressure and gas-pressure dominance inside the disk.

Key words: stars: neutron – pulsars: general – stars: magnetic fields.

1 INTRODUCTION

The discovery by *NuSTAR* (Bachetti et al. 2014) of coherent pulsations in the X-ray emission of an Ultra-Luminous X-ray source (ULX) has challenged our understanding of both ULXs as well as of accretion onto magnetized neutron stars (NSs). The source, observed at a peak X-ray luminosity L_X of $\sim 10^{40}$ erg s^{-1} (assuming isotropic emission) has triggered numerous studies aimed at discerning its nature and properties, and in particular the magnetic field strength of the accreting NS in it.

The early works, based on the value of the luminosity in this 'high-state', reached however conclusions which were not univocal. In particular, a magnetar-like magnetic field of $\sim 10^{14}$ G was derived by Eksi et al. (2014), while Lyutikov (2014) favoured a B-field $\sim 10^{13}$ G. A more 'typical' NS field of 10^{12} G was suggested by the analysis of Christodoulou et al. (2014; see also Bachetti et al. 2014), while Kluzniak & Lasota (2014) argued in favour of a very low field, $< 10^9$ G. A mixed magnetic field topology, with a low dipolar field and magnetar-strength multipoles was envisaged by Tong (2015). These different conclusions stemmed from the combination of different assumptions: i.e. isotropic emission versus beamed, spin equilibrium or else purely material accretion torques versus magnetically-threaded disks.

In Dall'Osso et al. 2015 (paper I from here on), we analyzed the source properties by considering a magnetically-threaded disk without prior assumptions on how close the NS is to spin equilibrium. Firstly, we used the average value of the period derivative $\dot{P}$ (over 4 sets of observations) to show that there exists a continuum of solutions in the B vs. $\dot{M}$ (or L_X) plane, and that the solutions found by previous investigators correspond to particular cases of the more general solution. Second, we included in the analysis the observed $\dot{P}$ variations to show that only high-field solutions, corresponding to $B \gtrsim 10^{13}$ G, could account for those fluc-

tuations (over four time intervals) without requiring major changes in $\dot{M}$, which would be at odds with the approximately constant X-ray emission of the source during the same time.

All these works relied on the NuSTAR J095551+6940.8 observations (Bachetti et al. 2014) of the source in its 'high' state, with $L_X \sim 10^{40}$ erg s^{-1}. However, an analysis of archival *Chandra* data over a period of 15 years by Brightman et al. (2015) revealed that the source can be found in several accretion states, with large luminosity variations, down to $L_X \sim$ a few $\times 10^{38}$ erg s^{-1}. In addition, Brightman et al. used *NuSTAR* data to study the spectrum of the pulsed component. They found it broadly consistent with typical spectra of accreting pulsars in High Mass X-ray Binaries (HMXBs). These archival *Chandra* observations were analyzed also by Tsygankov et al. (2015), who suggested a possible bimodal distribution of the luminosity, with two well-defined peaks separated by a factor ~ 40. They interpreted this bimodality as due to transitions between the accretion and the propeller phase in a NS with a magnetic field $\sim 10^{14}$ G.

Here, we begin by performing an analysis of two archival *Chandra/HRC* observations which were not previously published due to lack of spectral information. We show that, in one of those observations, the source was not detected. Hence, over the 15 years of observations, the source has displayed 3 states: a high-luminosity one with $L_X \sim 10^{40}$ erg s^{-1}, an intermediate-luminosity one with L_X varying between $\sim$ a few $\times 10^{38}$ erg s^{-1} to a few $\times 10^{39}$ erg s^{-1}, and a low-luminosity one with an upper limit of $L_X < 1.7 \times 10^{38}$ erg s^{-1} (see Sec. 2). These luminosity variations, which encompass the Eddington limit, also straddle the regime in which the inner disk transitions from being pressure-dominated to radiation-dominated. As such, the source NuSTAR J095551+6940.8 offers an unprecedented opportunity to study accretion onto a magnetized NS across a wide range of physical conditions. Such a study is the goal of this work.

The paper is organized as follows: Sec.2 describes the analysis of the relevant HRC *Chandra* data (where the source is not detected); Sec.3 summarizes the basics of the threaded disk model, both in the gas and in the radiation-dominated regimes. The direct application to NuSTAR J095551+6940.8 is presented in Sec.4 for a wide range of different models. We summarize and conclude in Sec.5.

2 CHANDRA ARCHIVAL OBSERVATIONS: SETTING A LIMIT ON THE LOWEST LUMINOSITY OF THE SOURCE

Brightman et al. (2015) analyzed *Chandra* archival observations covering a 15 yr period. A few of them were discarded either due to excessive contamination from nearby sources, or because no spectral information was available from the two unpublished long observations made with the HRC only. In the majority of the remaining cases, M82-X2 was detected revealing large flux variations, with the corresponding isotropic luminosity ranging from[1] $L_X \lesssim 10^{40}$ erg s^{-1} to $L_X \gtrsim (2-3) \times 10^{38}$ erg s^{-1}. For a few observations, Brightman et al. (2015) report detections at luminosities $\sim (1-2) \times 10^{38}$ erg s^{-1}, albeit with rather large relative errors. In addition to using these, here we also analyze the two long observations made with HRC in order to assess whether the source was actually detected and, if not, set an upper limit on its luminosity.

The HRC observations under consideration were performed on 2007 January 9 (Id. 8189 with a 61.3 ks exposure, Obs. 1 hereafter), and January 12 (Id. 8505 with an 83.2 ks exposure, Obs. 2 hereafter). In both cases *Chandra* observed M82 using the High Resolution Camera optimized for timing (HRC-S Timing). In order to eliminate mismatches in the absolute astrometry between the two observations, we reprojected them using the HRC Chandra image of the source region taken on October 28, 1999 (ObsId. 1411). We reduced and analyzed data with the Chandra Interactive Analysis of Observations (CIAO) version 4.7, and reprocessed event files using the CHANDRA_REPRO script, with the latest calibration files included in the CALDB v. 4.6.8.

We performed source detection by using the CIAO algorithm WAVDETECT (Freeman et al. 2002), which correlates the *Chandra* image with wavelets of different scales and searches for significant correlations. We searched at scales equal to 1.0, $\sqrt{2}$, 2.0, $2\sqrt{2}$, 4.0, $4\sqrt{2}$, 8.0, $8\sqrt{2}$, and 16.0 times the size of the pixel of HRC-S images (0.13 arcsec); some of these oversample the point spread function of an on axis point source (FWHM$\sim$ 0.4 arcsec). We set the detection threshold at the level expected to give at most one false source detection in the field that includes the brightest X-ray sources of the galaxy (green dashed box in Fig. 1).

Fig. 1 shows the image obtained during Obs. 1 (left panel) and Obs. 2 (right panel), respectively. NuSTAR J095551+6940.8 is barely detected, at a significance of 3.9σ, only during Obs. 2 (see the red circle in the right panel of Fig. 1, where the source is dubbed J095551.0, as in Table 2 of Chiang & Kong 2011). On the other hand, the source was undetected by WAVDETECT during Obs. 1. To estimate the photon counts in the two observations we used the CIAO routine SRCFLUX, extracting photons from a circle with a 0.9 arcsec radius (containing 90% of the counts expected from a point source) centered at the source position. The background was extracted from a larger region far from the center of the host galaxy. We obtain 0.1-10 keV count rates of $r_1 = (0.92 \pm 0.14) \times 10^{-3}$ and $r_2 = (1.55 \pm 0.15) \times 10^{-3}$ cts s^{-1} in Obs. 1 and 2, respectively.

Although the photon count (63) in Obs. 1 would lead to a detection in the absence of background diffuse emission close to the source position, wavelets at the considered scales did not show a significant correlation with the spatial count distribution. Hence we ascribe most of those counts to the diffuse emission of the galaxy. Indeed, extracting the flux from a circular region located just north-east of the the source location yields a count rate of $b_1 = (0.99 \pm 0.13) \times 10^{-3}$ cts s^{-1}, compatible with the flux observed from the position of M82-X2. The diffuse emission in the core of M82 varies by up to 70% in magnitude over spatial scales of ≈ 1.5 arcsec, and has an extremely patchy distribution: a reliable modelling of the diffuse emission appears prohibitive with present instrumentation. Therefore, since the relative contribution of the source and the diffuse emission to the observed flux is highly uncertain, we consider the observed val-

[1] Different spectral models cause slight luminosity differences.

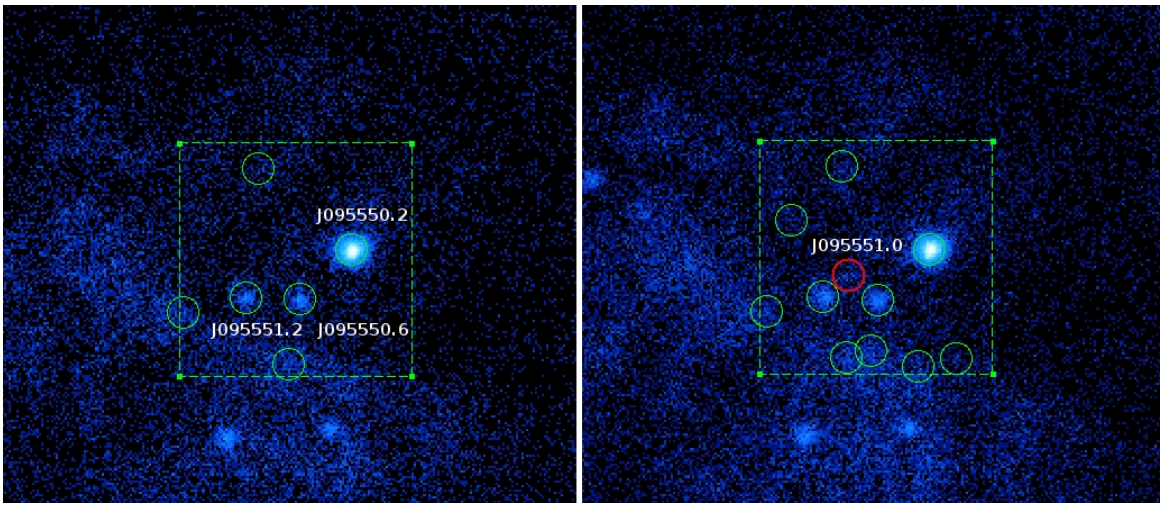

Figure 1. HRC-S image of the core of M28 obtained during Obs. 1 (left panel) and 2 (right panel), respectively. Green circles plotted with a radius of 0.9 arcsec indicate sources significantly detected by the wavelet algorithm used over the box indicated by the green dashed lines. A red circle in the right panel indicates the significant detection of NuSTAR J095551+6940.8.

Source	Obs. 1 (s^{-1})	Obs. 2 (s^{-1})
J095550.2	$(81.6 \pm 1.3) \times 10^{-3}$	$(81.0 \pm 1.0) \times 10^{-3}$
J095551.0	$(0.92 \pm 0.14) \times 10^{-3}$	$(1.55 \pm 0.15) \times 10^{-3}$
J095551.2	$(4.27 \pm 0.28) \times 10^{-3}$	$(4.98 \pm 0.26) \times 10^{-3}$
J095550.6	$(4.75 \pm 0.31) \times 10^{-3}$	$(4.70 \pm 0.25) \times 10^{-3}$

Table 1. Photon flux of the four sources in two different observations. J095551.0 (M82 X-2) was significantly detected only during Obs. 2.

ues as the most conservative upper limit on the source flux. Adopting the spectral parameters of the high-luminosity state of M82 X-2 (a power law with index $\Gamma = 1.33$ and absorption column of $N_H = 3.4 \times 10^{22}$ cm^{-2}; Brightman et al. 2015), the lowest observed count rate, r_1, translates into an unabsorbed (0.1-10) keV flux of 3.4×10^{-13} erg cm^{-2} s^{-1} and a luminosity of 4.4×10^{38} erg s^{-1} (at a distance of 3.3 Mpc; Foley et al. 2014). Alternatively, given that the count rate from the M82-X2 region in Obs. 1 was very close to that in neighbouring source-free regions, we also consider the possibility that r_1 is due to pure background emission. In this case, with a total background of 63 photons, we can place a 3σ upper limit of $\sim 0.38 \times 10^{-3}$ cts s^{-1} to the count rate at which the source would be statistically significant above the background. For the same spectral parameters as above, this translates into a (0.1-10) keV luminosity $\simeq 1.7 \times 10^{38}$ erg s^{-1} as a 3σ upper limit during Obs. 1 (ranging from 1.5 to 2.4 $\times 10^{38}$ erg s^{-1} for Γ = 1-2).

For the detection in Obs. 2 we proceeded as follows: if r_1 does indeed correspond to diffuse emission from the core of the galaxy, then the source contribution to r_2 will be $r_{src} = (0.63 \pm 0.2)$ cts s^{-1}. Again, adopting the same spectral parameters as above, r_{src} translates into a (0.1-10) keV luminosity of $\sim 2.7 \times 10^{38}$ erg s^{-1} in Obs. 2, consistent with the low-luminosity detections reported by Brightman et al. (2015). Indeed, when combined with those observations, our result strengthens the case for the lower (least conservative) upper limit discussed above for Obs. 1.

Two main conclusions can be drawn from our analysis of these additional *Chandra* observations, in combination with those reported by Brightman et al. (2015). The first is that the source is highly variable, ranging from a maximum luminosity $L_{peak} \gtrsim 10^{40}$ erg s^{-1} down to a minimum of $L_{min} \sim (2-3) \times 10^{38}$ erg s^{-1} (for a distance of 3.3 Mpc) where it can still be detected. Below the latter value, the background emission from the host galaxy becomes dominant and it is extremely hard to separate it from the emission of M82-X2. The second conclusion is that the source remained *undetected* in the first observation made with the HRC: we placed a very conservative upper limit of 4.4×10^{38} erg s^{-1} to the source luminosity during Obs. 1 – assuming that the entire count rate is due to the source – and a more stringent upper limit - based on a plausible assumption for the background - of $\sim 1.7 \times 10^{38}$ erg s^{-1}.

Whether this observed luminosity transition between Obs. 1 and 2 occurred in a continuous fashion or in a sharp step remains to be determined in the future, through deeper and less sparse observations of the source.

3 BASIC PROPERTIES OF MAGNETICALLY-THREADED DISKS

When accretion occurs onto a magnetic NS, the interaction between the accreting material and the NS magnetosphere affects the system dynamics in several ways. For disk accretion, in particular, the main elements can be briefly summarised as follows:

- The accreting plasma is threaded - at least partially - by the stellar magnetic field. The inner disk is truncated by the resulting magnetic stresses at a distance r_m from the NS. It is customary to write this truncation radius in terms of the classical Alfvén radius for spherical accretion, r_A, with the simple expression $r_m \simeq \xi r_A$, where $\xi < 1$. The Alfvén radius is where the magnetic pressure equals the ram pressure of the infalling material. It depends on the mass accretion rate,

$\dot{M}$, and on the NS mass, radius and magnetic moment[2]. For disk accretion, on the other hand, angular momentum balance is the most relevant constraint (see, e.g. Gosh & Lamb 1979, Wang 1996). At decreasing radii, the magnetic stress grows faster than the viscous/material one: once it becomes dominant, it disrupts the disk forcing matter to fall along magnetic field lines. This difference is simply encoded in the parameter ξ, the value of which is only weakly constrained: on observational grounds, a number of studies have indicated $\xi \sim (0.3-1)$ as a conservative estimate of the range of variation (Psaltis & Chakrabarty 1999). Theoretically, the semi-analytic model by Ghosh & Lamb 1979 (GL79 in the following), and recent numerical simulations (Romanova et al. 2002, 2003, 2004) indicate a value $\xi \approx 0.5$, with only a very weak dependence on $\dot{M}$, if any. In an alternative semi-analytic model, Erkut & Alpar (2004) estimate values of $\xi \sim 0.35-1.2$ in different sources, or even in the same source at different accretion stages. In an independent approach to the problem, Wang (1987, 1996) argued for a value of $\xi \gtrsim 1$; Bozzo et al. (2009) extended Wang's approach and showed that, in this model, r_m is almost independent of the mass accretion rate, over a wide range of values of $\dot{M}$. The relation with r_A in this case is more complex, involving an $\dot{M}$-dependent ξ (Sec. 4.3).

• The inner edge of the disk, r_m, depends on the total pressure inside the disk, which has a contribution from both gas and radiation. The relative importance of the latter grows at smaller radii, at a fixed mass accretion rate, as more energy is locally released inside the disk. In particular, for a given $\dot{M}$, one can define a transition radius, r_{tr}, inside which radiation pressure dominates over gas pressure (e.g., Frank et al. 2002):

$$r_{tr} \approx 7.5\times10^{7}\mathrm{cm}\left(\frac{\alpha}{0.1}\right)^{2/21}\left(\frac{\dot{M}}{\dot{M}_E}\right)^{16/21}\left(\frac{M}{1.4\mathrm{M}_\odot}\right)^{1/3}, \quad (1)$$

where α is the usual viscosity parameter and the Eddington mass accretion rate is $\dot{M}_E = 4\pi\sigma_T m_p R/c \approx 1.75\times10^{-8}M_\odot \mathrm{yr}^{-1}$, with the corresponding Eddington luminosity $L_E = GM\dot{M}_E/R \simeq 1.75\times10^{38}$ erg s^{-1}, for a 1.4 $M_\odot$ NS with a radius $R = 10$ km. As long as $r_{tr} < r_m$, only gas pressure is important in the disk. When $r_{tr} > r_m$, on the other hand, radiation pressure dominates the inner disk, where more energy is released and most of the disk-magnetosphere interaction occurs. Following this transition, a change in the functional form of r_m occurs and, in particular, a different dependence on $\dot{M}$ will ensue[3] (Ghosh 1996):

$$\begin{aligned} r_m^{(g)} &= \xi\left(\frac{\mu^4}{2GM\dot{M}^2}\right)^{1/7} \quad \mathrm{gas-pressure\ regime} \\ r_m^{(r)} &= A\left(\frac{\mu^4}{M\dot{M}}\right)^{1/7} \quad \mathrm{radiation-pressure\ regime}, \end{aligned} \quad (2)$$

where the magnetic dipole moment $\mu = B_p R^3/2$ and B_p is the field strength at the magnetic pole[4] . For consistency, the normalization, A, in $r_m^{(r)}$ is set so that the two expressions are equal at the transition radius, r_{tr}. As we will show in the next section, the weaker $\dot{M}$-dependence in radiation pressure dominated regions play an important role in NuSTAR J095551+6940.8.

• The threading magnetic field regulates the exchange of angular momentum between the NS and the disk. This exchange is characterized by two regions separated at the corotation radius, $r_{co} = (GM/\Omega_s^2)^{1/3}$, where the Keplerian frequency equals the NS spin frequency, Ω_s. In the *inner region* matter rotates faster than the NS, thus exterting a spin-up torque as it gives up angular momentum to the NS magnetosphere. In the *outer region* matter rotates slower than the NS, thus causing spin-down as it gains angular momentum from the faster rotating magnetosphere. Depending on the strength of these two terms, the NS can either spin-up or down while accreting; in either case, the system naturally evolves towards *spin equilibrium*, in which the magnetic and material torques are at equilibrium and the NS accretes at constant period. This occurs when $r_m^{(eq)} \approx (0.5-0.9)\, r_{co}$, depending on poorly known microphysical details of the disk-magnetosphere interaction (GL79, Wang 1987, 1996, Yi et al. 1997, Erkut & Alpar 2004, Parfrey et al. 2015). Spin equilibrium can be used to set a constraint on B_p, *if a transition between spin-up and spin-down is observed:* the luminosity at the transition yields the mass accretion rate at equilibrium, $\dot{M}_{eq}$, leaving only μ and ξ as unknowns in Eq. 2.

• The NS will be an *accretor* only if the disk extends inside the corotation radius, such that $r_m < r_{co}$. The accretion luminosity in this case is $L_{acc} \sim GM\dot{M}/R$. If, on the other hand, $r_m > r_{co}$, then matter cannot reach smaller radii than r_m: in approaching the faster rotating magnetosphere it acquires angular momentum and is thus forced outwards. This is the so-called *propeller regime*, in which accretion onto the NS is inhibited and a strong spin down is expected. Since matters doesn't flow inside r_m, only half of its potential energy at $r_m(\geq r_{co})$ is released, the other half remaining as kinetic energy of the orbital motion. The propeller luminosity is therefore $L_{prop} \leq GM\dot{M}/(2r_{co})$.

4 LUMINOSITY VARIATIONS IN NuSTAR J095551+6940.8: MODEL CONSTRAINTS

In the following we will use the observed luminosities of NuSTAR J095551+6940.8 to set constraints on the strength of the NS magnetic field and on the physical regime in the accretion disk.

The luminosity range over which the source is observed, from $\mathrm{L}_{\mathrm{min}}^{(ob)}$ to $\mathrm{L}_{\mathrm{peak}}^{(ob)}$, should correspond to the *accretor* phase, in which $r_m \lesssim r_{co}$ and the mass inflow proceeds all the way to the NS surface. Given the spin period and the magnetic dipole moment of the NS, this implies the existence of a minimum mass accretion rate, $\dot{M}_{min}$, below which r_m is larger than r_{co} and the NS enters the *propeller* regime.

The value of $\dot{M}_{min}$ and the associated luminosity, $\mathrm{L}_{min}^{(th)}$, are determined by the condition $r_m \equiv r_{co}$. This requires that we first set the value of the coefficient ξ in Eq. 2, and

[2] In more detailed calculations (e.g., Ghosh 1996, 2006) small corrections to this simple functional form were derived. These have only a minor effect on our estimates and, for the sake of simplicity, will be neglected in the following.

[3] The scaling with other physics parameters is mostly unaffected.

[4] Note that the above scalings cannot be used in the Wang model: we will show in Sec. 4.3, that this model can be described via a modified version of Eq. 2, with a specific $\dot{M}$-dependence of ξ that cancels out the one in the denominator.

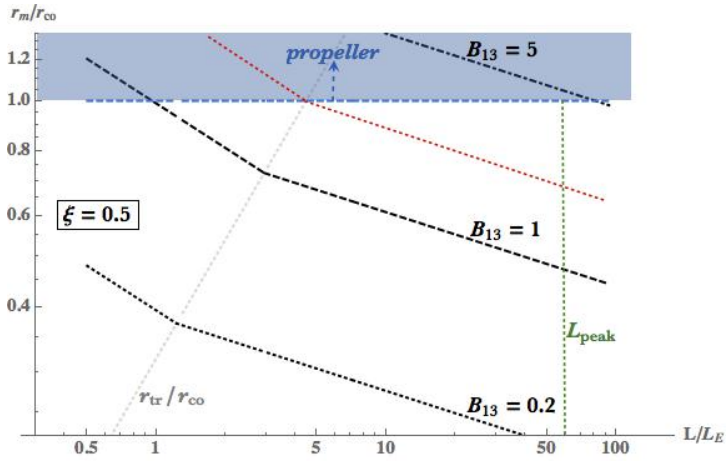

Figure 2. The ratio of the magnetospheric radius r_m and the corotation radius r_{co} as a function of the accretion luminosity, $L_{ac} = GM\dot{M}/R$, for three values of the magnetic field strength. The transition from the gas-pressure to the radiation-pressure dominated regime is indicated by the dashed grey line. The red dotted curve highlights the "special" case $B_{p,13} = 2$ (cf. Sec. 4.1).

then determine the pressure regime in the inner parts of the disk, which will select the appropriate expression for r_m. Given the uncertainties on ξ discussed in Sec. 3, we define here our "reference" model as the one with $\xi = 0.5$, close to the results of recent numerical simulations. This will be used for the core of our argument (Sec. 4.1), but then we will discuss the way our conclusions change if we let ξ vary within a wider range, from $\lesssim 0.3$ to 1 (Sec. 4.2). We will also consider a specific case in which ξ depends explicitly on $\dot{M}$. (Sec. 4.3). At the end of Sec. 4 we will summarize our main conclusions, showing that they remain robust against the use of widely different models for the disk-magnetosphere coupling.

4.1 The "reference model": $\xi = 0.5$

Using $\xi = 0.5$ in Eq. 2, we plotted in Fig. 2 the ratio r_m/r_{co} as a function of the accretion luminosity, $\mathrm{L}_{acc} = GM\dot{M}/R$, for three representative values of the dipole magnetic field. In the same figure we also show the transition radius, r_{tr}, as a grey dashed diagonal line: gas pressure dominates above that line, radiation pressure below it. Note that r_{tr}, hence the position of the grey dashed line, does not depend on the value of ξ. However, the value of the accretion rate at this transition, $\dot{M}_{tr}$, and of the associated luminosity, L_{tr}, are obtained from the equality $r_m^{(g)} = r_{tr}$, and thus depend (almost linearly) on ξ. In Eddington units we obtain

$$\frac{\dot{M}_{tr}}{\dot{M}_E} = \frac{L_{tr}}{L_E} \approx 3\ B_{p,13}^{6/11} (\xi/0.5)^{21/22} \frac{R_6^{18/11}}{M_{1.4}^{3/22}}\,, \qquad (3)$$

where $Q_x = Q/10^x$ and $M_{1.4} \equiv M/(1.4 M_\odot)$. By substituting $\dot{M}_{tr}$ in the condition $r_m^{(r)} = r_m^{(g)}$ one can fix the factor A in Eq. 2, obtaining $r_m^{(r)} = r_m^{(g)} (\dot{M}/\dot{M}_{tr})^{1/7}$.

Before describing in detail our results, three general conclusions can be drawn from the previous analysis:
1) If $B_{p,13} \lesssim 2$, the condition $r_m = r_{co}$ is reached in the gas-pressure dominated regime. This results from $\mathrm{L}_{min}^{(g)} < L_{tr}$, which readily yields $B_{p,13} < 2\ (\xi/0.5)^{-7/4} M_{1.4}^{35/96} R_6^{-37/16} (P_s/1.37)^{77/48}$. In this regime, the minimum accretion luminosity is

$$\frac{L_{min}^{(g)}}{L_E} \approx 0.96 B_{p,13}^2 \left(\frac{\xi}{0.5}\right)^{7/2} \left(\frac{P_s}{1.37}\right)^{-7/3} \frac{R_6^5}{M_{1.4}^{2/3}}\,. \qquad (4)$$

2) If $B_{p,13} > 2$, on the other hand, the disk is already radiation-pressure dominated at the propeller-accretor transition. In this case, the minimum luminosity has an even stronger dependence on the magnetic field, scaling like B_p^4, and is shifted towards larger values compared to the extrapolation of the gas-pressure dominated case.
3) If $B_{p,13} < 2$, the flattening of the $\dot{M}$-dependence of r_m beyond $\dot{M}_{tr}$ favours a much wider range of accretion luminosities than the standard $r_m \propto \dot{M}^{-2/7}$ scaling. On the contrary, the same flattening of the $\dot{M}$-dependence shrinks the range of accretion luminosities for NS with $B_{p,13} > 2$, because its effect is shifting the minimum upwards.

We can now look more closely at the behaviour of the solutions for three representative values of the magnetic field:

(i) For $B_{p,13} = 0.2$ the disk is radiation pressure-dominated at all accretion rates $\geq 1.1\ \dot{M}_E$, with the inner disk extending well inside the corotation radius. The observed luminosity range, $\sim (1.1 - 60)\ \mathrm{L}_E$, corresponds to r_m being between $\approx 0.22\ r_{co}$ and $\approx 0.4\ r_{co}$, always in the radiation-pressure dominated regime. Very close to the observed minimum, $L_{min}^{(ob)} \simeq 1.1 L_E \approx 2 \times 10^{38}$ erg s^{-1}, gas pressure takes over while the NS remains an accretor for further decreasing values of $\dot{M}$, until the transition to propeller coccurs at $L_{min}^{(th)} \approx 0.044\ \mathrm{L}_E (B_{p,12}/2)^2 (\xi/0.5)^{7/2} (\mathrm{P}_s/1.37\mathrm{s})^{-7/3}$. Due to the background emission from the host galaxy and the neighbouring sources, it will be observationally very challenging to track the source at these low luminosities; however, no sharp transition below the currently observed minimum is expected in this case.
At the same time, the high peak luminosity of the source would require a significant beaming if B $\sim 10^{12}$ G, since in this case there is no obvious way to exceed the Eddington limit by a large factor. In fact, a beaming ~ 0.15 would also reconcile the measured $\dot{P} \simeq 2 \times 10^{-10}$ with the (beaming-corrected) luminosity. Explaining such a beaming *of the pulsed emission* represents a problem on its own (see discussion in paper I). In addition, this scenario encounters an even greater difficulty in the large $\dot{P}$-fluctuations measured while the source was near its peak emission (Bachetti et al. 2014). This strongly suggest that the NS was close to spin equilibrium at that epoch (paper I), while the result $r_m \simeq 0.22\ r_{co}$ at the peak is hardly consistent with spin equilibrium, being largely below the range $r^{(eq)} \approx (0.5 - 0.95)\ r_{co}$ provided by all existing theoretical estimates. Therefore, a new explanation would also be required for the large $\dot{P}$ fluctuations.

(ii) For $B_{p,13} = 1$, radiation pressure dominates the inner disk at $\mathrm{L}_X \geq 3\ \mathrm{L}_E$, which corresponds to $r_m \leq 0.8\ r_{co}$; as expected, the disk is gas-pressure dominated at the minimum luminosity, $\mathrm{L}_{min}^{(g)} \approx 1.7 \times 10^{38}$ erg s^{-1} (cf. Eq. 4), similar to the currently observed minimum luminosity of M82-X2.

It is therefore a natural prediction that a spinning NS with $\mathrm{P}_s = 1.37$ s would be detectable as an accreting source down to $\sim 2 \times 10^{38}$ erg s^{-1} *if it had a magnetic dipole* $B \sim 10^{13}$ *G.*

Once in propeller, the luminosity will be much lower since

now the accretion radius will be r_{co} instead of R (e.g. Corbet 1996). In the case of an "ideal" (i.e. sharp) transition, the source luminosity should drop suddenly to $\sim 5{\times}10^{35}$ erg s^{-1}: even in a more realistic and smoother transition, a significant drop in luminosity must be expected just below the currently observed minimum (e.g., Romanova et al. 2003). More generally, an observational determination of L_{min} would allow a robust estimate of the magnetic field strength. In the observations discussed in Sec. 2 the source was undetected, with a 3σ upper limit on its luminosity of $\approx 10^{38}$ erg s^{-1}, consistent with $\mathrm{L}^{(g)}_{min}$ derived above: this limit can only be improved with future X-ray detectors having at least the same angular resolution of *Chandra* and a much larger collecting area (to achieve the required limit within reasonable exposure times), given the high and highly patchy background in the source region.

In addition, when B $\sim 10^{13}$ G the Eddington limit is significantly modified by the magnetically-reduced electron scattering cross-section, which gives a maximum luminosity $L^{(th)}_{peak} \sim 10^{40} B_{13}^{4/3}$erg s^{-1} (Paczynski 1992). This value matches well the observed peak luminosity of NuSTAR J095551+6940.8 (cf. paper I) that, as shown in Fig. 2, is naturally reached when $r_m \gtrsim 0.5 r_{co}$, a condition that is well consistent with spin equilibrium.

(iii) For $B_p \geq 5 \times 10^{13}$ G, the equality $r^{(r)}_m = r_{co}$ implies that the system is in the propeller regime at all accretion rates lower than $\sim 85\, \dot{M}_E (B_{p,13}/5)^4$. This limit, which is $\gtrsim 3$ times higher than what would have been obtained using $r^{(g)}_m$, is a direct consequence of the transition to the radiation-pressure dominated regime above $\dot{M} \sim 7.5\ \dot{M}_E$.

This "high-field case" is the most problematic in light of current observations. The NS can only enter the accretor regime at a minimum luminosity $\mathrm{L}^{(th)}_{min} \approx 1.7 \times 10^{40}$ erg s^{-1}, as a consequence of radiation pressure dominating the inner disk, thus violating two constraints at a time: on the one hand, $\mathrm{L}^{(th)}_{min}$ exceeds the observed peak luminosity of the source and, on the other hand, all intermediate states in which the source has a luminosity $\sim$ a few $\times 10^{39}$ erg s^{-1} would be impossible to account for, given that $\mathrm{L}_{prop} \sim 6 \times 10^{37}$ erg s^{-1}. A stronger field would only exacerbate this problem, given that $\mathrm{L}^{(th)}_{min}$ scales with B_p^4 in the radiation-pressure dominated regime. Note that, not accounting for the effects of radiation pressure would allow the NS to enter the accretor regime at a significantly lower luminosity, as was recently found by Tsygankov et al. (2015).

To summarize, we have shown that a NS with B $\sim 10^{13}$ G is sufficient to interpret the observational properties of NuSTAR J095551+6940.8 in a straightforward fashion: its peak luminosity, the minimum luminosity at which it is observed and the non-detections below that value. In addition, it was already shown that this case can also explain the measured value of $\dot{P}$ and its fluctuations around the peak luminosity (see Dall'Osso et al. 2015).
A lower field strength might not be excluded - although significantly lower B-fields require a high degree of fine-tuning (see paper I). A B-field significantly larger than 10^{13} G would not match the luminosity range over which the source is observed and can be ruled out.

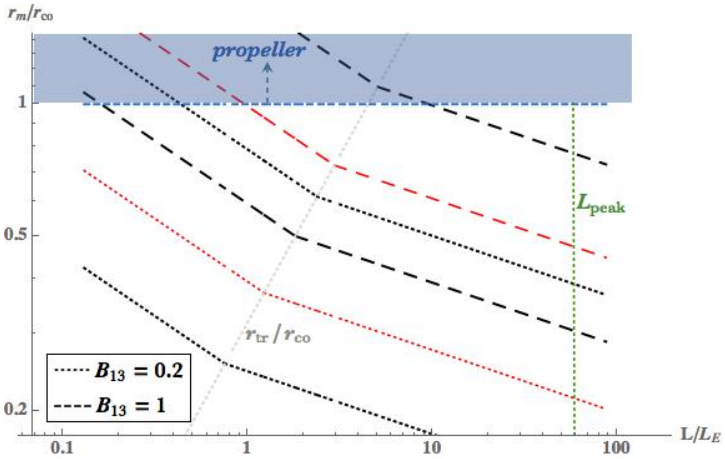

Figure 3. Same as in Fig. 2, but for different values of the parameter ξ. For each value of the magnetic field, the lower (dotted) black curve is obtained for $\xi = 0.3$ and the upper one (dashed) for $\xi = 1$. The red curves show the results of Fig. 2, obtained with the reference value $\xi = 0.5$.

4.2 Constant ξ models: dependence on ξ-values

We next explore the dependence of our results on the parameter ξ. Given the linear dependence of r_m on ξ, for the same magnetic field strength, a larger ξ will push the system in the propeller phase at larger values of $\dot{M}$. Correspondingly, the minimum luminosity at which the system can be in the accretion phase will be larger for larger ξ, given a fixed B-field strength. This is clear from the dependence of $\mathrm{L}^{(th)}_{min}$ on ξ in Eq. 4, and is shown in Fig. 3 for the two limiting cases $\xi = 0.3$ and $\xi = 1$. The dependence of $\dot{M}_{tr}$ on ξ (Eq. 3) is due to the shifting position of the r_m curves.

Conversely, we can rewrite Eq. (4) as a relation between the magnetic dipole of the source and the value of ξ, if we know the minimum luminosity at which the NS can accrete. Recalling that Eq. 4 holds for $B_{p,13} \lesssim 2$, we obtain

$$B_{p,13} \simeq \left[\frac{L^{(g)}_{min}}{L_E}\right]^{1/2} \left(\frac{\xi}{0.5}\right)^{-7/4} \left(\frac{P_s}{1.37s}\right)^{7/6} \frac{M_{1.4}^{1/3}}{R_6^{5/2}}\,. \qquad (5)$$

If we now assume for $L^{(g)}_{min}$ the minimum luminosity $L^{(ob)}_{min} \approx 10^{38}$erg s^{-1} determined with current observations (Sec. 2), then from Eq. 5 we obtain $B_{13} \sim (0.4 - 3)$ for ξ in the $(1 - 0.3)$ range, very similar to the "high-B case" discussed in paper I. These numbers can be easily adjusted if future observations will be able to determine the minimum luminosity with better accuracy: note, however, that the estimated magnetic field strength scales only with the square root of the minimum accretion luminosity.

4.3 Wang model: a specific prescription for $\xi(\dot{M})$

Wang (1987, 1995, 1996) derived the inner disk radius from the condition $r_m^2 B_z(r_m) B_\phi(r_m) = \dot{M}\left[d/dr\left(r^2\Omega_K\right)\right]_{r_m}$, *i.e.* that the magnetic stress is equal to the material stress in the disk[5]. Adopting different phenomenological prescriptions for

[5] The same condition is also considered in the GL model. However, in this model the radial rotation profile $\Omega(r)$ is allowed to deviate from keplerian in a narrow boundary layer, before reach-

the growth and dissipation of the toroidal field in the disk, the radial profile of $B_\phi(r)$ can be calculated and, hence, the value of r_m as a function of the NS magnetic field, the mass accretion rate and several microphysics parameters that are poorly constrained from both theory and observations.

This model predicts that, at spin equilibrium, the inner disk radius is close to the corotation radius ($r_m^{(eq)} \gtrsim 0.9 r_{co}$), nearly independent of the phenomenological prescriptions adopted for the toroidal field in the disk (Wang 1995). Bozzo et al. (2009) generalized this approach, deriving expressions for $x = r_m/r_{co}$ in Wang-type models with various prescriptions for the mechanisms by which the toroidal field is damped. Here we consider two cases, which bracket the (small) range of possible variations: *a)* the winding of the field lines threading the disk is limited by magnetic reconnection taking place in the magnetosphere; *b)* the amplification of the toroidal field is damped by diffusive decay due to turbulent mixing within the disk.

$$x^{-7/2} - x^{-2} = 4.17 \times 10^{-3} \frac{M_{1.4}^{5/3} P^{7/3} \dot{M}_{16}}{\gamma_{max}\ \eta^2 \mu_{30}^2} \quad a)$$

$$x^{-7/2} - x^{-2} = 4.17 \times 10^{-3} \frac{\alpha}{\gamma} \frac{M_{1.4}^{5/3} P^{7/3} \dot{M}_{16}}{\eta^2 \mu_{30}^2} \quad b)\ . \quad (6)$$

In the above, α is the usual viscosity coefficient, $\gamma = B_\phi/B_z$ is the magnetic pitch angle in the disk and γ_{max} its maximum value compatible with magnetic reconnection out of the disk plane, and η the factor by which the NS magnetic field is screened by electric currents flowing in the disk. These parameters are subject to significant uncertainties, that make it difficult to draw quantitative conclusions. However, such uncertainties can be bypassed *if a transition between spin-up and spin-down is observed* (Bozzo et al. 2009), since the transition signals the point of spin equilibrium. When expressed in terms of the equilibrium quantities, $\dot{M}_{eq}$ (observed) and $x^{(eq)}$ (fixed by the model), Eqs. 6 give x as a function of $\dot{M}$ and show that r_m remains $\lesssim r_{co}$, nearly constant for $\dot{M} < \dot{M}_{eq}$. In particular, accretion onto the NS continues even at the smallest values of $\dot{M}$, and is never quenched by the propeller. This apparently unphysical behaviour makes it impossible, within the framework of Wang-type models, to constrain the NS properties from luminosity variations. However, we can use Eqs. 6 to estimate the NS magnetic field based on the assumption that a spinup-spindown transition, or a very close approach to spin equilibrium, was observed in NuSTAR J095551+6940.8. This assumption is motivated by the large torque fluctuations measured by Bachetti et al. (2014), when the source was close to its peak luminosity (cf. paper I). We thus set[6] $\dot{M}_{eq} \approx 30 \dot{M}_E$, and use the value $x^{(eq)} \simeq 0.967(0.915)$ for case $a(b)$ in Eqs. 6 to obtain:

$$B_{p,13} \approx \frac{4.2}{\eta \gamma_{max}^{1/2}} \left(\frac{\dot{M}_{eq}}{30 \dot{M}_E}\right)^{1/2} P_{1.37}^{7/6} \frac{M_{1.4}^{5/6}}{R_6^3} \quad a)$$

$$B_{p,13} \approx \frac{0.9\ \alpha_{0.1}^{1/2}}{\eta \gamma^{1/2}} \left(\frac{\dot{M}_{eq}}{30 \dot{M}_E}\right)^{1/2} P_{1.37}^{7/6} \frac{M_{1.4}^{5/6}}{R_6^3} \quad b)\ . \quad (7)$$

These results are again in overall agreement with those of the previous sections and of paper I: as a general conclusion, the estimated $\sim 10^{13}$ G B-field appears robust against a variety of independent arguments and adopted models. Note that, since $\eta < 1$ and $\gamma \gtrsim 1$, slightly larger values of the magnetic field may possibly be favoured by Wang-type models.

Using the magnetic fields of Eqs. 7 we can calculate r_A and, since $r_m \lesssim r_{co}$ when $\dot{M} \lesssim \dot{M}_{eq}$, we obtain $r_m/r_A \sim (0.25 - 0.55)$ in NuSTAR J095551+6940.8, for $\dot{M} = (\dot{M}_E - \dot{M}_{eq})$. Eqs. 6 also imply that r_m starts decreasing approximately like r_A if $\dot{M} > \dot{M}_{eq}$ (Bozzo et al. 2009): therefore, ξ remains $\gtrsim 0.55$ when $\dot{M}$ is above the equilibrium value. As a conclusion, Wang's model may be cast in the form $r_m = \xi(\dot{M}) r_A$, where the numerical value of the function $\hat{\xi}(\dot{M})$ ranges in the lower half of the interval considered in the previous sections. This is consistent with our discussion of Sec. 4.2, that lower values of ξ tend to favour larger values of the NS magnetic field.

5 SUMMARY AND DISCUSSION

The wide spread of luminosities of NuSTAR J095551+6940.8 (M82-X2), encompassing a range from highly super-Eddington, to $\sim$ Eddington to no detection, has allowed to investigate various physically interesting accretion regimes for a magnetized NS.

Here, we have extended the analysis of archival *Chandra* data with the inclusion of two *HRC* observations. The source is detected in one of them, with an estimated luminosity $\sim 2.6 \times 10^{38}$ erg s^{-1}. On the other hand, the source is *undetected* in the first HRC observation, during which it is indistinguishable from the diffuse emission of the host galaxy. This non-detection yields a conservative upper limit of $L_{u.l.}^{(a)} \gtrsim 4.4 \times 10^{38}$ erg s^{-1} to the source luminosity, assuming that the background contribution to the counts from the M82-X2 region is negligible. On the other hand, by assuming that those counts are mostly due to the background - as suggested by the count rate being the same as in nearby background regions - we placed a more stringent upper limit of $L_{u.l.}^{(b)} \simeq 1.7 \times 10^{38}$ erg s^{-1} to the source luminosity.

We performed an in-depth analysis of the large luminosity variations of NuSTAR J095551+6940.8 (M82-X2), within a magnetically-threaded disk model, including the transition of the inner disk between gas-pressure and radiation-pressure dominance across the various accretion states. We explored a range of models characterized by different prescriptions for the location of the disk truncation radius, and found that the NS magnetic field should be in the (0.4-3)$\times 10^{13}$ G range, with a favored value of $\sim 10^{13}$ G, if accretion onto the NS becomes inhibited below a luminosity $\simeq L_E$. The latter value is fully compatible with the currently determined minimum luminosity of the source, and with the upper limit $L_{u.l.}^{(b)}$ discussed above. The estimated B-field is

ing the inner disk edge in corotation with the magnetosphere. This different treatment results in a different location of the inner disk edge in the GL model and a more pronounced dependence of r_m on the mass accretion rate.

[6] In paper I it was shown that the spinup-spindown transition is likely to occur at luminosities somewhat smaller than the peak. Hence, we set for reference this transition at half the peak, *i.e.* at 30 $\dot{M}_E$. Note the weak dependence of the estimates in Eq. 7 on the exact value of this parameter.

consistent with the conclusions of paper I, which were based on independent arguments.

In our analysis, the estimated magnetic field has a degeneracy with the poorly constrained value of ξ, the ratio between the disk truncation radius and the Alfvén radius. An independent determination of the NS B-field might in principle break this degeneracy, allowing to place interesting constraints on ξ, hence on the viability of different models for the disk-magnetosphere coupling. In accreting X-ray pulsars, one possible way to estimate the NS magnetic field is via a high-energy break in the emission spectrum, which is known to correlate with the cyclotron energy. However, the cyclotron resonance shifts to progressively lower energies in several bright X-ray pulsars, as the accretion luminosity grows and approaches the Eddington limit. This shift is attributed to the increasing height of the accretion column above the NS surface, which therefore samples regions of progressively decreasing B-field strength (Becker et al. 2012, and references therein). In NuSTAR J095551+6940.8, a spectral break at ~ 14 keV was detected when the source was close to its peak emission (Brightman et al. 2015): taken at face value, this is consistent with the break observed in several accreting NS with $B \sim 10^{12}$ G. However, we note that NuSTAR J095551+6940.8 is an extremely bright X-ray pulsar in an unprecedented accretion regime. If this trend, and the correlation between cyclotron energy and spectral break, were to continue into the super-Eddington regime, then $B_p \sim 10^{13}$ G may well be consistent with the finding of Brightman et al. (2015). In fact, revealing a shift in the spectral break energy of NuSTAR J095551+6940.8 when the source is at different luminosities would provide significant support to this idea.

ACKNOWLEDGEMENTS

SD was partially supported by an SFB/Transregio 7, funded by the Deutsche Forschungsgemeinschaft (DFG).
RP and SD acknowledge partial support by Chandra grant (awarded by SAO) ARS-16005X.

REFERENCES

Bachetti, M. et al. 2014, Nature, 514, 202
Becker, P. A., Klochkov, D., Schönherr, G., et al. 2012, A & A, 544, A123
Brightman, M. et al., 2015 arXiv150706014
Bozzo, E., Stella, L., Vietri, M., Ghosh, P. 2009, A&A, 493, 809
Christodoulou, D. M., Laycock, S. G. T., Kazanas, D. 2014, arXiv1411.5434
Corbet, R. H. D. 1996, ApJ, 457L, 31
Dall'Osso, S., Perna, R., Stella, L. 2015, MNRAS, 449, 2144 (paper I)
Eksi, K. Y., Anda, I. C., Cikintoglu, S., Gencali, A. A., Gungor, C., Oztekin, F. 2014, arXiv1410.5205
Erkut, M. H., Alpar, M. A. 2005, ApJ, 620, 390
Foley, R. et al. 2014, MNRAS, 443, 2887
Frank, J., King, A., Raine, D., 2002, Accretion Power in Astrophysics, ISBN 0521620538. Cambridge, UK: Cambridge University Press
Ghosh, P. 2007, Rotation and Accretion Powered Pulsars: World Scientific Series in Astronomy and Astrophysics – ISBN-13 978-981-02-4744-7. Published by World Scientific Publishing Co., Pte. Ltd., Singapore.
Ghosh, P. 1996, ApJ, 459, 244
Ghosh, P., Lamb, F. K. 1979, ApJ, 234, 296
Kluzniak, W., Lasota, J.-P. 2014, arXiv1411.100
Lyutikov, M. 2014, arXiv1410.8745
Parfrey, K., Spitkovsky, A., Beloborodov, A. M. 2015, arXiv150708627
Psaltis, D. & Chakrabarty, D. 1999, ApJ, 521, 332
Romanova, M. M., Ustyugova, G. V., Koldoba, A. V., Lovelace, R. V. E. 2002, ApJ, 578, 420
Romanova, M. M., Toropina, O. D., Toropin, Yu. M., Lovelace, R. V. E. 2003, ApJ, 588, 400
Romanova, M. M., Ustyugova, G. V., Koldoba, A. V., Lovelace, R. V. E. 2004, ApJ, 616L, 151
Tong, H. 2015, arXiv1508.3115
Tsygankov, S. S., Mushtukov, A. A., Suleimanov, V. F., Poutanen, J. 2015, arXiv150708288
Yi, I. Wheeler, J. C., Vishniac, E. T. 1997, ApJ, 481L, 51
Wang, Y.-M. 1987, A&A, 183, 257
Wang, Y.-M. 1995, ApJ, 449L, 153
Wang, Y.-M. 1996, ApJ, 465L, 111